ARTICLE

BacFlash signals acid-resistance gene expression in bacteria

Di Wu[1], Wenfeng Qi[1], Wei Nie[1,2], Zhengyuan Lu [1], Yongxin Ye[1], Jinghang Li[1], Tao Sun[1], Yufei Zhu[1,2], Heping Cheng [1,2] and Xianhua Wang[1,2]

Intracellular pH (pH_i) homeostasis is crucial for cellular functions and signal transduction across all kingdoms of life. In particular, bacterial pH_i homeostasis is important for physiology, ecology, and pathogenesis. Here we report an exquisite bacterial acid-resistance (AR) mechanism in which proton leak elicits a pre-emptive AR response. A single bacterial cell undergoes quantal electrochemical excitation, termed "BacFlash", which consists of membrane depolarization, transient pH_i rise, and bursting production of reactive oxygen species. BacFlash ignition is dictated by acid stress in the form of proton leak across the plasma membrane and the rate of BacFlash occurrence is reversely correlated with the pH_i buffering capacity. Through genome-wide screening, we further identify the ATP synthase F_o complex subunit a as the putative proton sensor for BacFlash biogenesis. Importantly, persistent BacFlash hyperactivity activates transcription of a panel of key AR genes and predisposes the cells to survive imminent extreme acid stress. These findings demonstrate a prototypical coupling between electrochemical excitation and nucleoid gene expression in prokaryotes.

INTRODUCTION

Intracellular pH (pH_i) homeostasis is of paramount importance across all kingdoms of life because most proteins require an optimal pH_i to maintain their structures and functions.[1] In particular, single-cell organisms have developed sophisticated pH_i homeostatic systems to cope with acid or alkaline challenges from fluctuating and unpredictable environments. For instance, *Escherichia coli* (*E. coli*), an intestinal bacterium prefers a neutral environmental pH (pH_e) and uses the heavy pH_i buffering provided by weak acids and bases, such as phosphate groups, ammonia, and the side-chains of amino acids, as the first line of defense to protect itself against rapid pH_i swings induced by pH_e changes.[2,3] Sustained pH_e acidification activates programmed acid-resistance (AR) responses, including the up-regulation of transporters catalyzing active proton efflux, such as proton-pumping electron transport chain (ETC) complexes, proton-coupled ATPase, and cation-proton antiporters.[4–7] Meanwhile, metabolic remodeling gears up to consume excess intracellular protons by enlisting the glutamate-dependent AR system involving the decarboxylases GadA and GadB to decarboxylate glutamate, and the antiporter GadC to export the resultant γ-aminobutyric acid.[8–10] In addition, periplasmic chaperon proteins such as HdeA and HdeB contribute to AR by preventing acid-induced protein aggregation and facilitating protein refolding after pH_e neutralization.[11]

Proton signaling is also highly conserved and crucial in cellular bioenergetics and signal transduction. In prokaryotes, as well as eukaryotic mitochondria, respiration-coupled electron transfer and proton transport develop a proton electrochemical potential, which acts as a source of free energy for ATP synthesis.[12] Fed by the electron donors NADH and $FADH_2$, electron flow through the ETC in the eukaryotic mitochondrial inner membrane or prokaryotic plasma membrane drives outwardly proton pumping, building up the proton motive force ($\Delta\mu_{H+}$), which comprises both the membrane potential ($\Delta\Psi$) and the proton gradient components (ΔpH).[12] The re-entry of protons at F_1F_o-ATP synthase harvests the free energy of $\Delta\mu_{H+}$ for the synthesis of ATP. The plasma membrane of bacterial cells is not only an active site for proton signaling, but also the first line of defense against acid stress. It has been shown that, under extremely low pH_e, the bacterial cells flip electric potential to slow proton movement into the cell through repulsion.[13] Whether and how the bacterial plasma membrane can sense acid stress and then relay the signal to express the downstream protective genes remains unclear.

In the present study, we discover a novel form of electro-chemical excitation in single *E. coli* cells, termed "BacFlash", which composes a transient pH_i rise, membrane depolarization, and bursting production of reactive oxygen species (ROS). Importantly, we demonstrate that the BacFlash activity senses acid stress in the form of proton leak with the ATP synthase F_o complex subunit a as the putative proton sensor. Moreover, we show that persistent BacFlash hyperactivity serves as an early warning signal of imminent acid stress and activates the transcription of a panel of key AR genes at neutral pH_e, and thereby protects the cells against subsequent acid stress. These findings illustrate a prototypical coupling between electrochemical excitation and selective gene expression in prokaryotes.

RESULTS

BacFlash: electrochemical excitation in single *E. coli* cells

To investigate bacterial pH_i homeostasis and signaling, we expressed the genetically-encoded pH indicator ecliptic pHluorin[14] in BW25113 cells, a common *E. coli* strain (Fig. 1a; Supplementary

[1]State Key Laboratory of Membrane Biology, Beijing Key Laboratory of Cardiometabolic Molecular Medicine, Peking-Tsinghua Center for Life Sciences, Institute of Molecular Medicine, Peking University, Beijing 100871, China and [2]Research Unit of Mitochondria in Brain Diseases, Chinese Academy of Medical Sciences, PKU-Nanjing Institute of Translational Medicine, Nanjing, Jiangsu, China
Correspondence: Heping Cheng (chengp@pku.edu.cn) or Xianhua Wang (xianhua@pku.edu.cn)
These authors contributed equally: Di Wu, Wenfeng Qi, Wei Nie

information, Fig. S1a). Confocal imaging visualized pulsatile increases of fluorescence occurring randomly among cells bathed in M9 minimal medium (Fig. 1a, b; Supplementary information, Fig. S1a and Video S1), indicative of spontaneous pH_i transients in these bacterial cells. Individual pH_i transients exhibited a full duration at half maximum of 8.4 ± 0.3 s and reached a peak of $18\% \pm 1\%$ increase in fluorescence (Supplementary information, Fig. S1b), the latter corresponding to an alkalization of ~0.49 pH units based on in situ calibration (pKa ~ 7.26) (Supplementary information, Fig. S2). Similar pH_i transients were observed with pHtomato, another genetically-encoded pH indicator with a pKa ~ 7.8[15] (Fig. 1c). Similar events were detected in BW25113 cells bathed in LB medium (Supplementary information, Fig. S3). To further delineate this phenomenon, we stained E. coli cells with tetramethyl rhodamine methyl ester (TMRM) to measure membrane potential, or 7-dichlorodihydrofluorescein diacetate (DCF) to detect ROS. The staining appeared to be heterogeneous among the intact cells (Supplementary information, Fig. S4), due perhaps to the strong efflux activity of the bacteria.[16,17] Nonetheless, we acquired dual indicator measurements in the portion of successfully stained cells, and found that pH_i transients were accompanied by downward deflections of the TMRM signals (Fig. 1c) and by stepwise increases in the DCF signals (Fig. 1c). Interestingly, robust pH_i transients persisted in spheroplasts whose cell walls were removed by

lysozyme and EDTA treatment (Supplementary information, Fig. S5), indicating that neither the cell wall nor the periplasm of the bacterium is required for the biogenesis of pH_i transients. Spheroplasts displayed much improved dye staining, with about 80% cells stained by TMRM and 65% cells stained by DCF. In these dye-stained cells, we showed that almost all pH_i transients reported by pHluorin (97%) were accompanied with transient decrease of TMRM, and 67% pH_i transients reported by pHtomato cooccurred with stepwise increase of DCF signals (Supplementary information, Fig. S6). Overall, these results substantiate that pH_i rise, membrane depolarization, and ROS burst all occur concurrently and represent different aspects of a new type of electrochemical excitation in a single bacterial cell. We named it bacterial flash (BacFlash), in analogy to its eukaryotic counterpart called mitochondrial flash (mitoflash)[18–21] (see Discussion).

The rate of occurrence of BacFlashes was ~5 events/1000 μm^2/100 s in BW25113 cells (Fig. 1d). BacFlashes with nearly identical frequency and properties were also detected in three other E. coli strains, BL21(DE3), DH5α, and Top10 (Fig. 1d; Supplementary information, Fig. S1). In colonies growing on agarose pads, BacFlashes were confined to individual cells (Supplementary information, Fig. S7), with no sign of intercellular propagation. During cell division, however, we observed synchronous Bac-Flashes in both daughter cells until their complete separation (Supplementary information, Fig. S8). In filamentous E. coli cells produced by cephalexin treatment to prohibit division,[22,23] BacFlashes were synchronized along the entire length of 20–100 μm (Supplementary information, Fig. S9 and Video S2). Inhibiting respiration with KCN and dissipation of proton electrochemical gradients with the ionophore carbonyl cyanide 4-(trifluoromethoxy) phenylhydrazone (FCCP) both markedly repressed BacFlash activity (Fig. 1e), indicating a tight link between BacFlash biogenesis and respiration in the bacteria. Altogether, we conclude that BacFlashes represent a fundamental activity that is intertwined with core physiology of E. coli cells.

Buffering pH_i quenches BacFlashes
In search of physiological regulators of BacFlashes, we serendipitously found a striking 40-fold increase in BacFlash frequency when ammonium (20 mM) was removed from the M9 minimal medium (Fig. 2a, b; Supplementary information, Video S3). The BacFlash response to ammonium removal was fully reversible (Fig. 2a) and was common to all four strains examined (Fig. 2b). These hyperactive BacFlashes were sensitive to inhibition of respiration (Supplementary information, Fig. S10b), as was the case in the presence of ammonium (Fig. 1e). In the absence of ammonium, BacFlash amplitude was moderately increased and the duration remained unaltered, while basal pH_i was slightly decreased (with F_0 decreased by ~10% corresponding to ~0.2 units) (Supplementary information, Figs. S2 and S10a). That is, ammonium acts as a powerful inhibitor of the biogenesis of BacFlashes, operating mainly in a frequency-modulatory mode.

Because ammonium participates in bacterial nitrogen metabolism, we tested whether the ammonium inhibition of BacFlashes could be caused by altered nitrogen source availability. We found that replacing ammonium with equimolar glycine or glutamate in M9 minimal medium failed to prevent the hyperactivation of BacFlashes induced by ammonium removal (Supplementary information, Fig. S11a). Further, in the TCE-Glu (PKUW151) strain, which uses glutamate as the preferred nitrogen source,[24] glutamate did not suppress the hyperactive BacFlashes either (Fig. 2c). In 13 mutants with ammonia metabolic gene knockout, not only was basal BacFlash activity unaltered in the presence of ammonium, but also their responses to ammonium removal remained intact (Supplementary information, Fig. S11b). These three lines of evidence exclude bacterial nitrogen metabolism as the mechanism underlying the ammonium-induced inhibition of BacFlashes.
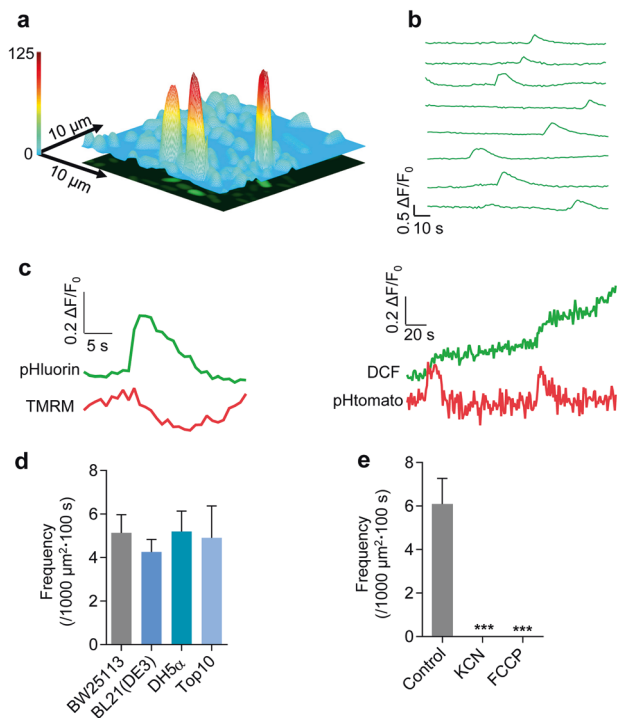

Fig. 1 Spontaneous electrochemical excitation termed "BacFlash" in single bacterial cells. Data were collected from BW25113 E. coli cells expressing pHluorin and bathed in M9 minimal medium, unless otherwise specified. **a** Surface plot of pHluorin-reported BacFlashes as peaks overlaying a confocal fluorescence image of rod-shaped cells. Three spontaneous events registered in 100-s periods are shown. **b** Traces of BacFlashes in cells with BacFlashes occurring. Each row represents BacFlash activities from a single cell in a 100-s period. **c** Membrane depolarization and ROS burst in a BacFlash reported by TMRM and DCF, respectively, with pHluorin or pHtomato reporting the pH_i transient. **d** BacFlash frequency in different E. coli strains. The frequency was indicated by quantifying the flash number in 1000 μm^2 of cell area in 100 s. Data are means ± SEM. $n = 17–27$ image stacks per group. **e** Inhibition of BacFlash activity by ETC blocker and an uncoupler. KCN (5 mM) for complex IV and the uncoupler FCCP (10 μM) were used. Data are means ± SEM. $n = 23–38$ image stacks per group. ***$P < 0.001$ vs control group.
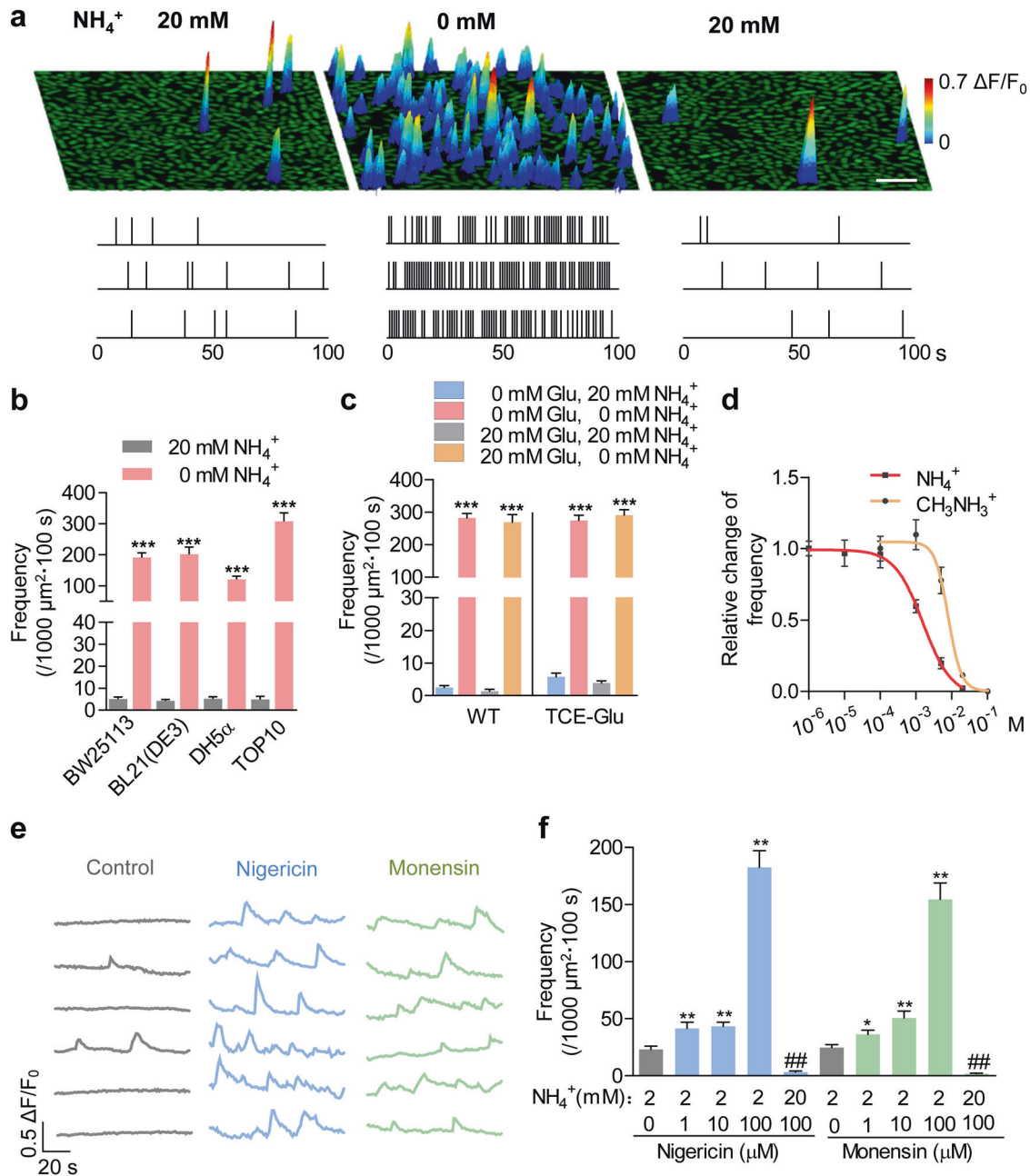
Fig. 2 Transmembrane proton leak triggers BacFlashes. a Ammonium removal from M9 minimal medium reversibly induced hyperactive BacFlashes. The images were taken in 5 min after ammonium removal or after ammonium re-addition. Upper panel, surface plots showing BacFlashes registered in 100-s periods overlaying the respective fluorescence background. Scale bar, 5 μm. Lower panel, raster plots of BacFlash incidence from three experiments in each group. Each tick denotes the occurrence of a BacFlash event. The top plot corresponds to the experiment shown in the upper panel. **b** Effects of ammonium removal on BacFlash frequency in different *E. coli* strains. $n = 6–27$ image stacks per group. ***$P < 0.001$ vs respective 20 mM ammonium group. **c** Ammonium, but not glutamate, inhibited BacFlash activity in the TCE-Glu strain, which prefers glutamate as a source for nitrogen metabolism. The wild-type (WT) strain PKUW13 was used as the control. Data are means ± SEM. $n = 12–14$ image stacks per group. ***$P < 0.001$ vs 20 mM ammonium group. **d** Both ammonium and methylammonium inhibited BacFlashes in a concentration-dependent manner. Note that methylammonium does not enter the bacterial nitrogen metabolism pathway. $IC_{50} = 1.56$ mM for ammonium and 7.91 mM for methylammonium. Data are means ± SEM. $n = 5–16$ image stacks per data point. **e** BacFlashes induced by the proton antiporters nigericin (100 μM) and monensin (100 μM). In the control group, ammonium was set at 2 mM to support a moderate rate of BacFlash activity. **f** Concentration-dependent effects of nigericin and monensin on activating BacFlashes. Data are means ± SEM. $n = 9–42$ image stacks per group. *$P < 0.05$, **$P < 0.01$ vs respective control group. ##$P < 0.01$ vs 100 μM nigericin or monensin group.

Considering that ammonium can enter the cytosol and act as a weak base (pKa ~ 9.33),[6] we then hypothesized that the inhibition of BacFlashes by ammonium might reflect its pH_i buffering capacity. In this regard, methylammonium ($CH_3NH_3^+$), which can also enter the cytosol as a pH_i buffer (pKa ~ 10.73) but does not

participate in bacterial nitrogen metabolism,[25,26] showed a concentration-dependent suppression of BacFlashes with an IC_{50} of 7.91 mM (Fig. 2d), while quantitative analysis of ammonium inhibition of BacFlashes yielded an IC_{50} of 1.56 mM (Fig. 2d). The higher IC_{50} value for methylammonium over ammonium is

consistent with its relatively lower pH buffering capacity in the physiological pH range (7.4–7.8 in *E. coli*[6,27]). When present at high concentrations, both pH buffers completely abolished BacFlash activity, indicating that pH$_i$ buffering quenches BacFlash biogenesis. Moreover, the inverse correlation between BacFlash frequency and pH$_i$ buffering capacity suggests possible involvement of BacFlashes in signaling AR response.

Free protons trigger BacFlashes

Microscopically, increasing pH$_i$ buffering would shorten the lifespan of a free proton and the distance it traverses before it is re-bound. That pH$_i$ buffers repress BacFlash activity in a concentration-dependent manner suggests that free protons might serve as the predominant trigger for BacFlash biogenesis in *E. coli* cells. Since basal pH$_i$ decreased only mildly (~0.2 pH units) (Supplementary information, Fig. S10a) even when BacFlash frequency swung over orders of magnitude (Fig. 2a, b), it is also clear that global pH$_i$ is unlikely to be the most critical determinant of BacFlash ignition; instead, free protons that trigger BacFlashes must be highly localized to microdomains, presumably at putative proton-sensing sites. To test the hypothesis that local free protons trigger BacFlashes, we treated *E. coli* cells with nigericin or monensin, which are antibiotics mediating electroneutral H$^+$/K$^+$ or H$^+$/Na$^+$ antiport and can deliver nascent free protons at the inner surface of the plasma membrane without perturbing the membrane potential.[21] We showed that, starting from a moderate basal frequency set by 2 mM ammonium, nigericin and monensin effectively elicited BacFlashes in a concentration-dependent manner, reaching 6.8- and 5.2-fold increases at 100 μM nigericin and monensin in intact *E. coli* cells, respectively (Fig. 2e, f). Again, pH$_i$ buffering with 20 mM ammonium profoundly inhibited the BacFlash activity induced by these proton antiporters (Fig. 2f). In the absence of cell walls, these proton antiporters appeared to be much more efficacious, with similar BacFlash-triggering effects achieved at about two orders of magnitude lower concentrations in spheroplasts than intact cells (Supplementary information, Fig. S12). Together with BacFlash-quenching effect of pH$_i$ buffers, these results substantiate the idea that free protons near the inner surface of the plasma membrane act as the predominant trigger of BacFlashes.

The ATP synthase F$_o$ complex subunit a serves as a putative sensor for BacFlash biogenesis

Next, we sought to identify putative proton sensors responsible for BacFlash ignition by undertaking a genome-wide screening of the Keio collection of *E. coli* knockouts.[28] The screening was performed in ammonium-free M9 minimal medium allowing for high BacFlash activity (Fig. 3a), and a computer algorithm modified from FlashSniper[29] was used to automatically detect BacFlashes in massive image datasets (see Materials and methods). Two criteria were set for a putative proton sensor-knockout mutant: it would display a dramatically lower BacFlash frequency and would no longer respond to antiporter-introduced proton trigger. Out of 3985 non-essential knockout mutants in the collection, 3281 mutants successfully expressed the indicator pHluorin and were used for three rounds of screening (see Materials and methods). At a cut-off value of 70% decrease in BacFlash frequency, we identified 128 candidates in the first round (Supplementary information, Fig. S13a), confirmed 34 candidates in the second round (Supplementary information, Fig. S13b), and finally pinpointed three candidate genes, *atpB*, *cyaA*, and *argO* (Fig. 3b). We then applied nigericin (100 μM) to further assess the mutants for their responsiveness to artificially-introduced proton trigger. Strikingly, we found that *atpB*-knockout completely abolished the nigericin-induced BacFlash activity (Fig. 3c). In contrast, nigericin still significantly enhanced the BacFlash activity in the *cyaA*- and *argO*-knockout mutants, albeit at smaller magnitudes (Fig. 3c). These results indicate that only *atpB* satisfies

both criteria for a putative proton sensor, whereas *cyaA* and *argO* appear to play regulatory, rather than obligatory, roles in BacFlash biogenesis.

AtpB encodes subunit a of the F$_o$ sector of the membrane-bound ATP synthase which interacts with subunit c to form a ring-like structure obligatory to both the ATP synthase and ATPase activities.[30,31] Interestingly, subunit c deficiency had little effect on BacFlash frequency (fold change of 1.07 ± 0.08 compared to the wild-type). Because both subunit a and c are essential for ATP synthase and ATPase activity, these results indicate that the *atpB*-mediated regulation of BacFlash biogenesis depends on neither ATP synthase/ATPase activity nor ATP synthesis-coupled proton influx.

Hyperactive BacFlashes time-dependently activate AR gene expression and protect the cells against acid stress

During a BacFlash, transient pH$_i$ rise, which is likely through enhancing ETC complex-mediated proton efflux, accounts for an immediate relief of acid stress and the transient membrane depolarization can also slow down the proton leak, suggesting that BacFlashes may constitute a novel AR mechanism. The question arising is whether and how the BacFlash mechanism is integrated into the sophisticated AR system developed in the single-cell organisms. To further appraise possible role of BacFlashes in bacterial AR response, we performed RNA-sequencing analysis under conditions of either hyperactive or hypoactive BacFlash activity. In particular, we investigated whether BacFlashes can regulate the expression of AR genes of different classes. Among 4040 *E. coli* genes analyzed, only 52 (~1.3%) were up-regulated and 47 (~1.2%) were down-regulated in cells displaying hyperactive BacFlashes compared with their counterparts in which BacFlash activity was inhibited by either 20 mM ammonium or 20 mM methylammonium (Supplementary information, Table S1). Bioinformatic analysis revealed that the genes up-regulated by ≥5 folds in hyperactive BacFlash group were highly enriched in multiple pH response pathways (Supplementary information, Fig. S14). In particular, the AR genes of multiple classes, including those in glutamate metabolism (the structural components *gadA*, *gadB*, and *gadC* and the central regulator *gadE*), the AR membrane protein (*hdeD*), and AR chaperones (*hdeA* and *hdeB*), were enriched (Fig. 4a). Using the lacZ assay, we further assessed the kinetics of the promoter activation of these induced AR genes.[32] At low BacFlash activity with either 20 mM ammonium or methylammonium (Supplementary information, Fig. S15), the promoters of these AR genes all remained quiescent (Fig. 4b). After switching to ammonium-free M9 minimal medium, persistent hyperactivity of BacFlashes time-dependently activated these AR genes with a latency of ~1.5 h and a half-time of activation of 2.4–3.0 h in wild-type cells (Fig. 4b; Supplementary information, Fig. S15). Furthermore, in the *atpB*-knockout mutant, which lacks the putative proton sensor for BacFlash biogenesis and displays low BacFlash activities (Fig. 3b, c), none of the aforementioned AR genes was activated by switching from ammonium- or methylammonium-containing to ammonium-free M9 minimal medium (Fig. 4b). Functionally, we found that hyperactive BacFlashes induced with ammonium removal conferred the wild-type bacterial cells higher survival rates in response to acid stress (Fig. 4c), however, the *atpB*-knockout mutant showed high vulnerability to acid stress under all experimental conditions tested (Fig. 4c). It is noteworthy that this newly-identified AR mechanism operated at neutral pH$_e$ (7.4) and is accompanied by only a small change in pH$_i$ (~0.2 units) (Supplementary information, Fig. S10a), in sharp contrast to the AR response induced by an extremely acidic pH$_e$ (2.0–4.0).[8–10] These results indicate that the BacFlash-activated AR gene expression serves as an early-warning signal, preconditioning bacterial cells to better survive imminent acid stress. Thus, the newly identified BacFlash-mediated AR mechanism senses an imbalance between
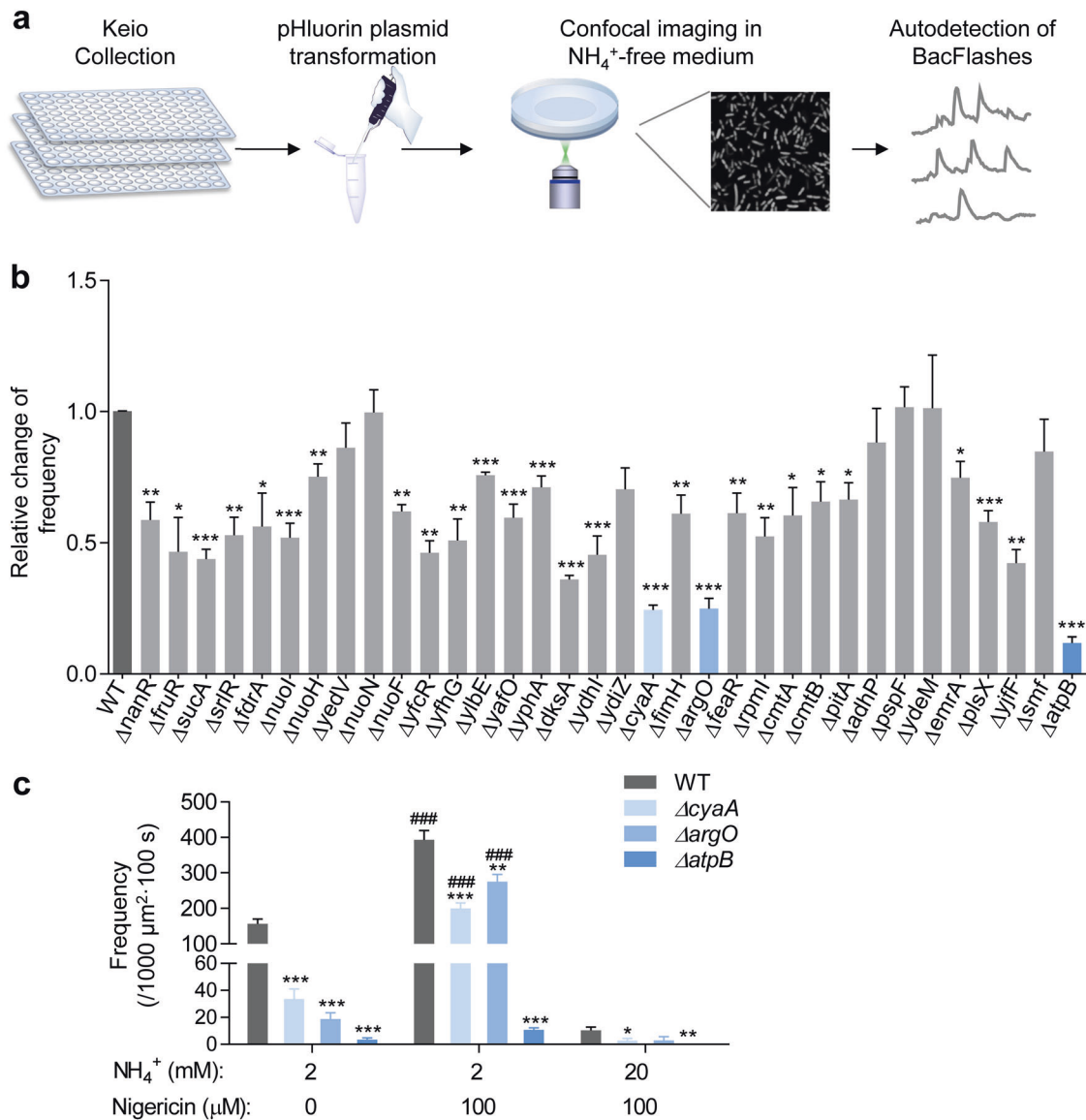
Fig. 3 Identification of putative proton sensor *atpB* for BacFlash ignition. a Schematic diagram for whole-genome screening of BacFlash regulators in the Keio collection of BW25113 knockouts. See Materials and methods for details. **b** Relative BacFlash frequencies in different mutants from the third round of screening. The frequency in each mutant was normalized to WT frequency. Data are means ± SEM. $n = 3–16$ image stacks per group. *$P < 0.05$, **$P < 0.01$, ***$P < 0.001$ vs WT. **c** Loss of BacFlash response to nigericin (100 μM) in *atpB*-knockout mutant. Data are means ± SEM. $n = 4–12$ image stacks per group. *$P < 0.05$, **$P < 0.01$, ***$P < 0.001$ vs WT group under the same conditions. ###$P < 0.001$ vs 0 μM nigericin group in the same *E. coli* strain.

proton leak and pH$_i$ buffering, and preemptively activates the expression of a panel of key AR genes prior to overt acidosis.

DISCUSSION

We have shown that single *E. coli* cells undergo quantal and stochastic electrochemical excitation in the form of BacFlashes, which can be directly visualized by different indicators for pH$_i$, membrane potential, or ROS. Multiple processes take place simultaneously in a BacFlash: sudden membrane depolarization likely involves the gating of one or a few membrane channels, transient pH$_i$ rise may reflect accelerated proton efflux by ETC operating at depolarized membrane potential, and ROS burst may arise from massive diversion of electrons from the ETC to the reaction with oxygen. Recently, transient membrane depolarization has been reported in single *E. coli* cells expressing an optical voltage sensor proteorhodopsin.[17,33] However, this type of

membrane depolarization differs from BacFlashes in several important ways. First, in contrast to conscious pH$_i$ rise in a BacFlash, no pH$_i$ changes[17] or a very small pH$_i$ decrease (< 0.1 pH units)[33] was detected among these previous reported events. Second, increasing laser illumination augments the frequency and abbreviates the duration of the proteorhodopsin-reported events,[17] but exerts little effects on the frequency as well as time course of BacFlashes (Supplementary information, Fig. S16). Thus, BacFlashes and the proteorhodopsin-reported events are mechanistically different and BacFlashes represent a previously unappreciated type of prokaryotic cellular dynamics.

On the other hand, BacFlashes bear remarkable resemblances to the eukaryotic mitoflashes that we and others reported previously.[18–21,34] Spontaneous mitoflash in respiring mitochondria, also comprises an action potential-like mitochondrial depolarization, a transient rise in matrix pH, and bursting production of ROS. Mitoflashes of similar properties prevail among
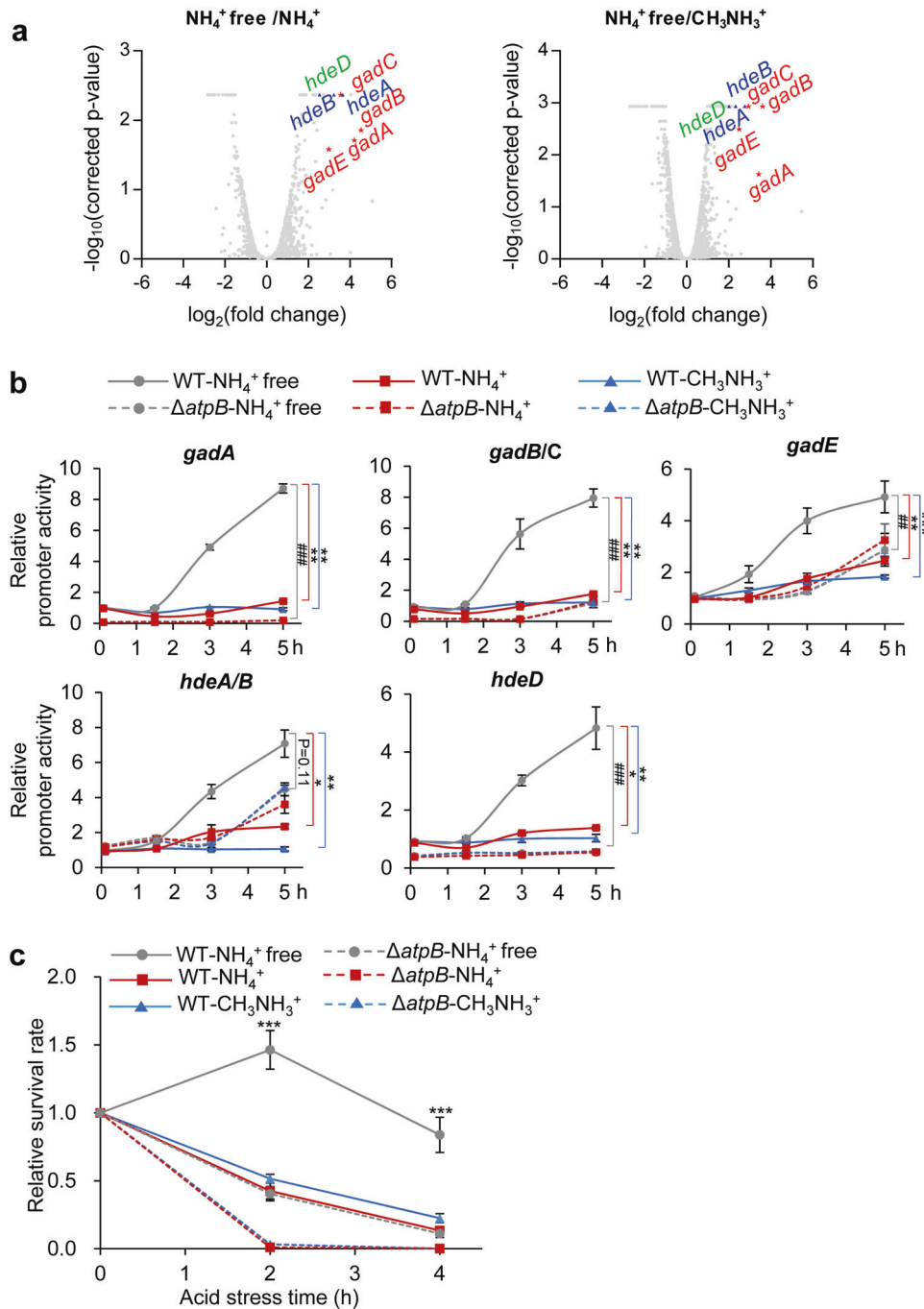
Fig. 4 Hyperactive BacFlashes time-dependently activate the expression of a panel of key AR genes. a Volcano plots showing the relative transcript abundance of genes measured by RNA-sequencing under conditions of high or low BacFlash activity. The glutamate metabolism-mediated AR genes (*gadA*, *gadB*, *gadC*, and *gadE*, marked in red), AR membrane protein (*hdeD*, green), and AR chaperones (*hdeA* and *hdeB*, blue) were activated at the transcriptional level in the BacFlash high-activity group (ammonium-free M9 minimal medium for 5 h) relative to the low-activity groups (M9 minimal medium containing 20 mM ammonium or methylammonium). **b** Time-dependent promoter activation of the AR genes in response to hyperactivity of BacFlashes. Both the WT and *atpB*-knockout mutant were in ammonium-free M9 minimal medium (WT-NH_4^+ free or *atpB*-NH_4^+ free), or M9 minimal medium containing 20 mM ammonium (WT-NH_4^+ or *atpB*-NH_4^+), or M9 minimal medium containing 20 mM methylammonium (WT-$CH_3NH_3^+$ or *atpB*-$CH_3NH_3^+$). The promoter activities at different time points in different groups were normalized to that of WT-NH_4^+ group at 0 h. Note that ammonium removal failed to activate AR gene expression in the *atpB*-knockout mutant. Data are means ± SEM. $n = 3$ independent experiments per group. $*P < 0.05$, $**P < 0.01$, $***P < 0.001$, ammonium-free M9 minimal medium group vs 20 mM ammonium or methylammonium group in WT; $^{\#\#}P < 0.01$, $^{\#\#\#}P < 0.001$, *atpB*-knockout vs WT in ammonium-free M9 minimal medium. **c** Survival rates of WT and *atpB*-knockout cells in response to acid stress. The survival rates were normalized to that of 0 h point in each group. Data are means ± SEM. $n = 14–16$ replicates from 4 independent experiments per group. $***P < 0.001$ vs 20 mM ammonium or methylammonium of WT cells at the same time point.

all eukaryotes examined[18–21] and even in isolated mitochondria,[35–37] indicating that it is a highly conserved and autonomous property of the organelle. Transient opening of mitochondrial permeability transition pore (mPTP), which is known as a megachannel in mitochondrial inner membrane,[38] has been reported to be tightly coupled with mitoflash generation, evidenced by precipitous dissipation of mitochondrial membrane potential and irreversible loss of small solutes from the matrix in a mitoflash.[18,19] We hypothesize that similar megachannel may exist in bacterial plasma membrane and its transient and reversible opening might account for transient depolarization of membrane potential in a BacFlash. Although the molecular identity of mPTP is still in debate, it has been proposed that ATP synthase might be one of the mPTP candidates.[38,39] In this regard, the present finding that subunit a of ATP synthase acts as a putative proton sensor for BacFlash generation is in line with an intimate relationship between mPTP and ATP synthase. Since the mitochondrion is thought to have originated from an alpha-proteobacterial ancestor through endosymbiosis,[40] it is conceivable that electro-chemical excitation in the form of BacFlash might represent an evolutionarily ancient physiological activity in prokaryotes that has been essentially conserved in eukaryotes, assuming the form of mitoflash.

It has been shown that mitoflashes fulfill an elemental signaling role in a cell type-specific and context-sensitive manner, regulating mammalian cardiac ATP homeostasis,[41] participating in skeletal muscle metabolism,[42] and signaling structural long-term potentiation of neuronal synapses.[43] In the present study, we find that BacFlash biogenesis confers a new AR mechanism on bacterial cells by acting as an early warning signal. Differing from previously characterized AR mechanisms, the BacFlash-mediated AR appears to specifically respond to a new form of acid stress-sustained proton leak that is unbalanced by intracellular pH buffers. First, an inverse relationship between BacFlash frequency and pH_i buffering capacity was uncovered. BacFlash displays low frequency under normal culture medium containing heavy pH buffers, however, when changing the pH_i buffering capacity by varying the concentration of ammonium or methylammonium with the pH_e unchanged, the BacFlash frequency varied over orders of magnitude and vanished at high pH_i buffer capacity, even though the pH_i changed only mildly (~0.2 units). This testifies a high signal-to-background contrast and high signal-to-noise ratio for BacFlash frequency to decode proton leak, a predictor of imminent acid stress. Second, proton leak induced by the electroneutral H^+/K^+ antiporter nigericin or the H^+/Na^+ antiporter monensin ignited hyperactive BacFlashes, and this trigger effect can also be abolished by pH_i buffering. More importantly, through genome-wide screening of the Keio collection of E. coli knockouts, we showed that the ATP synthase F_o complex subunit a encoded by atpB meets the two criteria we set for a putative proton sensor for BacFlash generation: it is obligatory for both spontaneous and proton antiporter-induced BacFlashes. It should be noted that the atpB-mediated proton ignition of BacFlashes depends on neither ATP synthase/ATPase activity nor ATP synthesis-coupled proton influx because the F_oF_1-ATP synthase subunit c deficiency had little effect on BacFlash frequency. These results are in general agreement with the finding in mammalian cells that proton leak triggers mitoflashes over a nanometer scale.[21]

It appears that this newly identified AR mechanism is well integrated with the sophisticated bacterial AR system for both short-term and long-term responses. BacFlashes would slow down the proton leak owing to the membrane depolarization and enhance proton efflux as manifested by the pH_i rise, both of which would immediately relieve acid stress. More importantly, Bac-Flashes relay the acid stress signal to nucleoid gene expression, activating the transcription of multiple classes of AR genes in a coordinated, time-dependent manner. These AR genes include the key components of glutamate metabolism (gadA, gadB, gadC, and

gadE), the AR membrane protein (hdeD), and AR chaperones (hdeA and hdeB). The BacFlash-activated expression of these AR genes effectively preconditions the bacterial cells to resist and survive subsequent acid stress. In addition to the immediate and long-term responses, our data also suggest an indirect mode of action for the BacFlash-mediated AR mechanism. In the genome-wide screen, we also identified two other BacFlash regulators that partake the AR response: cyaA and argO. Specifically, cyaA encodes an adenylate cyclase catalyzing the synthesis of the second messenger cyclic AMP, and its deficiency results in pH-sensitive growth impairment in E. coli.[44] ArgO encodes an arginine transporter mediating arginine export, further supporting the role of BacFlash biogenesis in pH_i homeostasis. Overall, we have demonstrated that the BacFlash AR mechanism operates at neutral pH_e (7.4), in sharp contrast to the AR response induced by an extremely acidic pH_e (2.0–4.0),[8–10] and teleologically, serves as an early warning signal to preemptively activate an AR response prior to overt cellular acidosis.

MATERIALS AND METHODS

Reagents
Nigericin, monensin, DCF, FCCP, lysozyme, methylamine hydrochloride ($CH_3NH_2 \cdot HCl$), sodium dodecyl sulfate, Na_2CO_3, $CaCl_2$, Na_2HPO_4, NaH_2PO_4, KH_2PO_4, KCl, NaCl, $MgSO_4$, $MgCl_2$, NH_4Cl, ampicillin, kanamycin, and chloramphenicol were from Sigma-Aldrich (Missouri, USA). 2-Mercaptoethanol was from Merck Millipore (Darmstadt, Germany). Polylysine was from Solarbio (Beijing, China). L-glutamic acid monosodium salt, D-glucose, and sucrose (RNA-free) were from VWR Life Science AMRESCO (Pennsylvania, USA). L-glutamine was from BioDee Biotechnology (Beijing, China). CCCP and 2-nitrophenyl β-D-galactopyranoside were from MedChemExpress (New Jersey, USA). Isopropyl β-D-thiogalactoside (IPTG) was from Thermo Fisher Scientific (Massachusetts, USA).

E. coli strains
The E. coli strains used in this study are listed in Supplementary information, Table S2. BL21(DE3) and BW25113 are in regular use in our laboratory. Top10 and DH5α were bought from TransGen Biotech (Beijing, China). PKUW13 and PKUW151 were gifted by Prof. Yi-Ping Wang of Peking University. Glycerol stocks were maintained at −80 °C, and individual colonies were picked for each experiment. The single gene-knockout mutants were from the Keio collection.[28] Each strain carries a non-essential gene replaced with a kanamycin resistance cassette.

Construction and expression of pHluorin and pHtomato
The genes for super-ecliptic pHluorin (GenBank: AF058694.2)[14] and pHtomato (GenBank: JQ966306.1)[15] were cloned into pTricHisA (Thermo Fisher Scientific, Massachusetts, USA) using the BamHI and HindIII restriction sites. The plasmid containing pHluorin or pHtomato was transfected into E. coli cells. A colony of cells from a fresh solid Luria-Bertani (LB) plate was inoculated into LB medium for overnight growth at 37 °C with shaking at 250 rpm for pre-culture. The next day, the pre-culture was diluted 1:100 into fresh LB medium as the experimental culture. Cells were grown to the early-log phase ($OD_{600} = 0.3$–0.4), 0.2 mM IPTG was added, and growth was allowed to continue further. The cells were harvested after 1 h for further experimentation.

Preparation of filamentous E. coli and spheroplasts
Filamentous E. coli and spheroplasts were prepared from E. coli strain BW25113 as described previously.[22] Briefly, BW25113 cells were transformed with pHluorin, and a colony of cells was inoculated into 5 mL LB medium for overnight growth at 37 °C with shaking at 250 rpm, then diluted 1:100 in the same medium and grown to OD_{600} 0.5–0.7. This culture (3 mL) was then diluted

1:10 in LB medium and cephalexin was added to 60 µg/mL. The culture was then shaken for 2–2.5 h at 37 °C until single-cell filaments reached sufficient length (20–150 µm).

These filamentous cells were harvested by centrifugation at 1500 × g for 2 min, and the pellet was rinsed without resuspension by the gentle addition of 1 mL 0.8 M sucrose solution and then allowed to rest at room temperature (22–26 °C) for 1 min. The supernatant was then removed with a Pasteur pipette and discarded, and the pellet was re-suspended in 2.5 mL 0.8 M sucrose. To remove the cell wall, the following reagents were added in order: 150 µL of 1 M Tris-HCl (pH 7.8); 120 µL of lysozyme (5 mg/mL); 30 µL of DNase I (5 mg/mL); and 120 µL of 0.125 M Na-EDTA (pH 8.0). This mixture was incubated at room temperature for 4–8 min to hydrolyze the peptidoglycan layer. At the end of this incubation, 1 mL of a solution containing 20 mM $MgCl_2$ (to remove the EDTA and activate the DNase), 0.7 M sucrose, and 10 mM Tris-HCl (pH 7.8) was added slowly (over 1 min) while stirring, and the mixture was incubated at room temperature for four more minutes. The mixture containing spheroplasts was either used immediately or kept at −20 °C.

Confocal imaging of BacFlashes

E. coli cells grown in LB medium at 37 °C were harvested by centrifugation. The harvested cells were placed on 1% agarose pads (low melting-point agarose was added to the M9 minimal medium above to a final concentration of 1% weight/volume then heated until the agarose dissolved) or polylysine-coated glass slides (a 0.01% weight/volume solution of polylysine was dropped on the glass slides and dried in the hood) for confocal imaging. For polylysine adhesion, the *E. coli* cells were left to adhere to these slides put in 6-well plate for 5 min in M9 minimal medium and centrifuged at 4000 rpm for 15 min, followed by washing three times with M9 minimal medium to remove non-adhered cells. All experiments were carried out at room temperature, except for monitoring growth on the agarose pad, which was performed at 37 °C.

An inverted confocal microscope (Zeiss LSM 710) with a 40×, 1.3 NA oil-immersion objective was used for imaging. When imaging pHluorin alone, images were captured by excitation at 488 nm and the emission was collected at > 505 nm. For pHtomato imaging, images were captured by exciting at 543 nm and collecting the emission at > 550 nm. For TMRM measurements, the indicator (100 nM) was loaded at 37 °C for 20 min. Images were captured by exciting at 543 nm and collecting the emission at > 550 nm. To acquire pHluorin and TMRM signals simultaneously, images were acquired by alternating excitation at 488 and 543 nm and emission collection at 500–530 and > 560 nm, respectively. For DCF measurements, the indicator (25 µM) was loaded at 37 °C for 20 min followed by washing three times with M9 minimal medium. For staining of the spheroplasts, the DCF (25 µM) was kept in the bath solution during imaging. The DCF fluorescence imaging was performed by exciting at 488 nm and collecting emissions at > 500 nm, with a low laser intensity to minimize photochemical reactions of DCF. To record DCF and pHtomato simultaneously, images were acquired by alternating excitation at 488 and 543 nm and emission collection at 500–530 nm and > 560 nm, respectively.

In typical time-lapse recordings of BacFlashes, 100 frames of 512 × 512 pixels were collected at 1.58 µs/pixel in bidirectional scanning mode. The frame rate was 1 frame/s, and the axial resolution was set to 1.0 µm. All cells were imaged within 1 h of treatment, and all experiments were performed at room temperature unless specified otherwise.

In situ calibration of pHluorin

In pHluorin-expressing BW25113 cells, 200 µM CCCP was used to break down pH gradients across the cell membrane and was present throughout all experimental conditions. The first recording of pHluorin fluorescence was made in M9 minimal medium at pH_e 8.0. After changing the medium to the designated experimental pH_e, the pHluorin fluorescence was recorded and then normalized to the pH_e 8.0 recording. The averaged normalized fluorescence values at different pH_e values were fitted to a Hill curve to obtain the pKa and the Hill coefficient of pHluorin in situ.

RNA sequencing analysis

BW25113 cells at log phase ($OD_{600} = 0.12$) in M9 minimal medium were centrifuged and re-suspended in ammonium-free M9 minimal medium supplemented with 20 mM sucrose, 20 mM ammonium, or 20 mM methylammonium. After treatment for 5 h at 37 °C with shaking at 250 rpm, total RNA was extracted using an RNAprep pure Cell/Bacteria kit (Tiangen, Beijing, China). RNA sequencing was then performed on an Illumina Hiseq 2500 platform (San Diego, California, USA), and 101-bp paired-end reads were generated for each treatment regimen.

The BW25113 genome and annotation files were downloaded from GenBank for the following analysis.[45] To obtain the genes differentially expressed between cells with different levels of BacFlash activity, the reads were first preprocessed to evaluate the data quality and rRNA rate and then aligned to the *E. coli* genome with Bowtie2.[46] The reads with high mapping quality (≥ 30) were normalized to calculate gene expression levels using FPKM (Fragments per Kilobase per Million mapped reads). Specific regions were used to represent gene loci to exclude the influence of overlapped regions in the gene expression calculation. Cuffdiff was used to obtain differentially expressed genes with cutoffs of fold-changes > 2 or < 0.5 and *P* values < 0.05. Two data sets from two independent biological replicates were merged to obtain the final up- or down-regulated genes. The genes up-regulated by ≥ 5 folds were bioinformatically analyzed using KOBAS3.0. The RNA sequencing data are available at https://www.ncbi.nlm.nih.gov/sra/PRJNA656061 and the NCBI accession number is PRJNA656061.

Promoter activity assay

The promoter regions of the target genes, as described previously[47] (Supplementary information, Table S3), were amplified from MG1655 genomic DNA using High-Fidelity DNA polymerase (NEB, Massachusetts, USA) and inserted into the pMP190 plasmid (gifted by Prof. Yi-Ping Wang, Peking University) using the *XbaI* and *KpnI* restriction sites. The inserted sequence was checked by sequencing. The BW25113 cells transformed by promoter-containing plasmid were cultured to the log phase ($OD_{600} = 0.4$) in M9 minimal medium, centrifuged, and then re-suspended in ammonium-free M9 minimal medium supplemented with 20 mM sucrose, 20 mM ammonium, or 20 mM methylammonium. At different time points (0.1, 1.5, 3, and 5 h), the cells (~5 mL of cell culture) were collected and frozen on dry ice. The promoter activity was assessed as described previously.[48] Briefly, 200 µL *ortho*-nitrophenyl-β-galactoside was added to 1 mL cell lysate, and the reaction was stopped within 5 min by adding 0.5 mL 1 M Na_2CO_3. A colorimetric assay at 420 nm was performed using an ultraviolet spectrophotometer (Shimadzu, Kyoto, Japan), and the promoter activity was calculated as $OD_{420}/min/mL/OD_{600}$ as follows:

$$\text{Activity} = \frac{OD_{420}}{OD_{600} \times \text{Time(min)} \times \text{Volum(µL)}} \times 1000$$

Acid resistance assay

The acid resistance assay was performed after overnight growth (18 h) of BW25113 cells in the LB medium. Briefly, the overnight culture was diluted 1:10 into M9 minimal medium and cultured for 2 h at 37 °C with shaking. The cells were then centrifuged and re-suspended in ammonium-free M9 minimal medium supplemented

with 20 mM sucrose, 20 mM ammonium, or 20 mM methylammonium and cultured for 5 h at 37 °C with shaking. After adjusting cell densities according to their OD_{600} value, the cells were suspended in M9 medium without ammonium, pH 2.0, and incubated for 0, 2, and 4 h, separately, at 37 °C with shaking. Then the cells were diluted 1:5000 in LB medium, plated to LB agar, and incubated at 37 °C for 15 h before colony counting. The survival rates were reported by normalizing the colony numbers after 2 or 4 h acid challenge to those at 0 h in each group.

Genome-wide screening of BacFlash regulator genes
The single gene-knockout mutants (3985 nonessential knockout mutants) used for genome-wide screening were from the Keio collection.[28] Briefly, each strain was transformed with pHluorin-containing plasmid and induced to express pHluorin by 0.2 mM IPTG. After 1.5 h of induction, the E. coli cells were centrifuged onto polylysine-coated slides in M9 minimal medium for confocal imaging. For each strain, the images were first captured in 20 mM ammonium-containing M9 minimal medium and then in ammonium-free M9 minimal medium. The image data were obtained in at least 3 regions from each condition. In the first-round screening, mutants showing ≥ 70% decrease of BacFlash frequency were considered as candidates for putative proton sensor genes. These candidates were then examined in a second-round screen using the same protocols and with ≥ 50% decrease of BacFlash frequency. A total of 3281, 128, and 34 mutants were used in the first, second, and third rounds of screening, respectively, and > 15,000 time-lapse image stacks of 512 × 512 × 100 pixels were generated.

Automated BacFlash detector
The automated detector of BacFlashes was modified from our previous Flashsniper for mitoflashes.[29] The overall detection scheme was divided into three steps: (1) image pre-processing to de-noise and eliminate motion artifacts, (2) cell edge-extraction by segmentation, and (3) event detection and parametric extraction.

Image pre-processing. We used a 5-kernel Gaussian-blur for image de-noising, and motion artifacts were eliminated through image registration. The Fourier-Mellin transformation[49] was used to estimate the motion parameters between the reference and target images. Considering that movement within an image stack was often slow and continuous, we fitted the frame-by-frame estimated parameters with a quadratic function over the entire stack. The inter-frame movements were then corrected accordingly, using the fitted parameters.

Cell edge-extraction. A comprehensive thresholding method combining global and local thresholds was used for segmentation. The global threshold was determined by Otsu thresholding.[50] The local threshold for each pixel was the average value of its local neighbors within a defined window centered at that pixel[51,52]:

$$T_{ij} = \frac{1}{MN} \sum_{m=-M/2}^{M/2} \sum_{n=-N/2}^{N/2} f(i+m, j+n)$$

where $f(i, j)$ is the intensity at pixel (i, j), and T_{ij} is the corresponding threshold. MN is the size of the neighborhood window. When the pixel intensity was higher than the global threshold, its threshold was set to the global threshold, otherwise it was set to the local threshold of the corresponding pixel. Then a binary image was computed with the calculated threshold:

$$T_{final}^{ij} = \begin{cases} T_{otsu}, f(i,j) < T_{otsu} \\ T_{ij}, \text{otherwise} \end{cases}$$

where T_{otsu} is the global Otsu threshold and T_{ij} is the local threshold at pixel (i, j).

To segment overlapped cells, the binary image was further processed by distance transformation and gray reversal.[53] After basic smoothing, watershed segmentation was implemented on the reversed distance transform image.[54–56] The resultant watersheds were used to split the overlapped regions. To avoid over-segmentation, neighboring sub-regions were merged if their temporal correlation coefficient ρ was > 0.5.

Event detection and parametric extraction. We obtained the time course of pHluorin or pHtomatto fluorescence signals for each segmented E. coli cell. An algorithm for BacFlash event detection started with the location of a local peak in the signal. An event was detected when the peak was larger than its previous m points with a threshold T_1 and n following points with a threshold T_2 per the following formula:

$$f_i > \max(f_{i-m} : f_{i-1}) + T_1 \,\&$$
$$f_i > \max(f_{i+1} : f_{i+n}) + T_2$$

The window size was $m + n$. We set $m = 3$, $n = 3$ and $T_1 = 0.01 \times$ maxima of the curve. Once identified, the event parameters basal fluorescence (F_0), peak ($\Delta F/F_0$), full duration at half maximum, and rise time were measured based on the time courses of BacFlashes. The BacFlash frequency was indicated by quantifying the flash number in 1000 μm^2 of cell area in 100 s.

Statistics
Data are expressed as the means ± SEM. When appropriate, Student's t-test was applied to determine the statistical significance of differences. In the promoter activity assay, one-way ANOVA was used to determine the significance of differences between three or more group sets. A two-tailed $P < 0.05$ was considered statistically significant.

AUTHOR CONTRIBUTIONS
D.W., W.Q., W.N., Z.L., and Y.Z. performed experiments. Y.Y., J.L., and T.S. developed algorithms and software for automated BacFlash detection. X.W. and H.C. conceived and supervised the project and wrote the manuscript with inputs from all co-authors.

ADDITIONAL INFORMATION
Supplementary information accompanies this paper at https://doi.org/10.1038/s41422-020-00431-3.

Competing interests: The authors declare no competing interests.

REFERENCES
1. Talley, K. & Alexov, E. On the pH-optimum of activity and stability of proteins. *Proteins* **78**, 2699–2706 (2010).
2. Rius, N., Sole, M., Francia, A. & Loren, J. G. Buffering capacity and H+ membrane conductance of gram-negative bacteria. *FEMS Microbiol. Lett.* **130**, 103–110 (1995).
3. Casey, J. R., Grinstein, S. & Orlowski, J. Sensors and regulators of intracellular pH. *Nat. Rev. Mol. Cell Biol.* **11**, 50–61 (2010).
4. Foster, J. W. *Escherichia coli* acid resistance: tales of an amateur acidophile. *Nat. Rev. Microbiol.* **2**, 898–907 (2004).

712

5. Slonczewski, J. L., Fujisawa, M., Dopson, M. & Krulwich, T. A. Cytoplasmic pH measurement and homeostasis in bacteria and archaea. *Adv. Microb. Physiol.* **55**, 1–79, 317 (2009).

6. Krulwich, T. A., Sachs, G. & Padan, E. Molecular aspects of bacterial pH sensing and homeostasis. *Nat. Rev. Microbiol.* **9**, 330–343 (2011).

7. Kanjee, U. & Houry, W. A. Mechanisms of acid resistance in *Escherichia coli*. *Annu. Rev. Microbiol.* **67**, 65–81 (2013).

8. Smith, D. K., Kassam, T., Singh, B. & Elliott, J. F. *Escherichia coli* has two homologous glutamate decarboxylase genes that map to distinct loci. *J. Bacteriol.* **174**, 5820–5826 (1992).

9. De Biase, D., Tramonti, A., Bossa, F. & Visca, P. The response to stationary-phase stress conditions in *Escherichia coli*: role and regulation of the glutamic acid decarboxylase system. *Mol. Microbiol.* **32**, 1198–1211 (1999).

10. Hersh, B. M., Farooq, F. T., Barstad, D. N., Blankenhorn, D. L. & Slonczewski, J. L. A glutamate-dependent acid resistance gene in *Escherichia coli*. *J. Bacteriol.* **178**, 3978–3981 (1996).

11. Hong, W., Wu, Y. E., Fu, X. & Chang, Z. Chaperone-dependent mechanisms for acid resistance in enteric bacteria. *Trends Microbiol.* **20**, 328–335 (2012).

12. Nicholls, D. G. & Ferguson, S. L. Bioenergetics. (Academic Press, London, 2002).

13. Richard, H. & Foster, J. W. *Escherichia coli* glutamate- and arginine-dependent acid resistance systems increase internal pH and reverse transmembrane potential. *J. Bacteriol.* **186**, 6032–6041 (2004).

14. Miesenbock, G., De Angelis, D. A. & Rothman, J. E. Visualizing secretion and synaptic transmission with pH-sensitive green fluorescent proteins. *Nature* **394**, 192–195 (1998).

15. Li, Y. & Tsien, R. W. pHTomato, a red, genetically encoded indicator that enables multiplex interrogation of synaptic activity. *Nat. Neurosci.* **15**, 1047–1053 (2012).

16. Bohnert, J. A., Karamian, B. & Nikaido, H. Optimized Nile Red efflux assay of AcrAB-TolC multidrug efflux system shows competition between substrates. *Antimicrob. Agents Chemother.* **54**, 3770–3775 (2010).

17. Kralj, J. M., Hochbaum, D. R., Douglass, A. D. & Cohen, A. E. Electrical spiking in *Escherichia coli* probed with a fluorescent voltage-indicating protein. *Science* **333**, 345–348 (2011).

18. Wang, W. et al. Superoxide flashes in single mitochondria. *Cell* **134**, 279–290 (2008).

19. Hou, T., Wang, X., Ma, Q. & Cheng, H. Mitochondrial flashes: new insights into mitochondrial ROS signalling and beyond. *J. Physiol.* **592**, 3703–3713 (2014).

20. Wang, W. et al. Mitochondrial flash: integrative reactive oxygen species and pH signals in cell and organelle biology. *Antioxid. Redox Signal* **25**, 534–549 (2016).

21. Wang, X. et al. Protons trigger mitochondrial flashes. *Biophys. J.* **111**, 386–394 (2016).

22. Martinac, B., Buechner, M., Delcour, A. H., Adler, J. & Kung, C. Pressure-sensitive ion channel in *Escherichia coli*. *Proc. Natl. Acad. Sci. USA* **84**, 2297–2301 (1987).

23. Perozo, E. Gating prokaryotic mechanosensitive channels. *Nat. Rev. Mol. Cell Biol.* **7**, 109–119 (2006).

24. Wang, J., Yan, D., Dixon, R. & Wang, Y. P. Deciphering the principles of bacterial nitrogen dietary preferences: a strategy for nutrient containment. *MBio* **7**, e00792–16 (2016).

25. Yoch, D. C., Zhang, Z. M. & Claybrook, D. L. Methylamine metabolism and its role in nitrogenase "switch off" in Rhodopseudomonas capsulata. *Arch. Microbiol.* **134**, 45–48 (1983).

26. Jayakumar, A., Epstein, W. & Barnes, E. M. Jr Characterization of ammonium (methylammonium)/potassium antiport in *Escherichia coli*. *J. Biol. Chem.* **260**, 7528–7532 (1985).

27. Lund, P., Tramonti, A. & De Biase, D. Coping with low pH: molecular strategies in neutralophilic bacteria. *FEMS Microbiol. Rev.* **38**, 1091–1125 (2014).

28. Baba, T. et al. Construction of *Escherichia coli* K-12 in-frame, single-gene knockout mutants: the Keio collection. *Mol. Syst. Biol.* **2**, 2006.0008 (2006).

29. Li, K. et al. Superoxide flashes reveal novel properties of mitochondrial reactive oxygen species excitability in cardiomyocytes. *Biophys. J.* **102**, 1011–1021 (2012).

30. Fillingame, R. H. & Steed, P. R. Half channels mediating H(+) transport and the mechanism of gating in the Fo sector of *Escherichia coli* F1Fo ATP synthase. *Biochim. Biophys. Acta.* **1837**, 1063–1068 (2014).

31. Allegretti, M. et al. Horizontal membrane-intrinsic alpha-helices in the stator a-subunit of an F-type ATP synthase. *Nature* **521**, 237–240 (2015).

32. Miller, J. H. Experiments in Molecular Genetics. (Cold Spring Harbor Laboratory Press, New York, 1972).

33. Bruni, G. N., Weekley, R. A., Dodd, B. J. T. & Kralj, J. M. Voltage-gated calcium flux mediates *Escherichia coli* mechanosensation. *Proc. Natl. Acad. Sci. USA* **114**, 9445–9450 (2017).

34. Breckwoldt, M. O. et al. Multiparametric optical analysis of mitochondrial redox signals during neuronal physiology and pathology in vivo. *Nat. Med.* **20**, 555–560 (2014).

35. Zhang, X. et al. Superoxide constitutes a major signal of mitochondrial superoxide flash. *Life Sci.* **93**, 178–186 (2013).

36. Wei-LaPierre, L. et al. Respective contribution of mitochondrial superoxide and pH to mitochondria-targeted circularly permuted yellow fluorescent protein (mt-cpYFP) flash activity. *J. Biol. Chem.* **288**, 10567–10577 (2013).

37. Feng, G. et al. Mitoflash biogenesis and its role in the autoregulation of mitochondrial proton electrochemical potential. *J. Gen. Physiol.* **151**, 727–737 (2019).

38. Bernardi, P., Rasola, A., Forte, M. & Lippe, G. The mitochondrial permeability transition pore: channel formation by F-ATP synthase, integration in signal transduction, and role in pathophysiology. *Physiol. Rev.* **95**, 1111–1155 (2015).

39. Carraro, M., Carrer, A., Urbani, A. & Bernardi, P. Molecular nature and regulation of the mitochondrial permeability transition pore(s), drug target(s) in cardioprotection. *J. Mol. Cell Cardiol.* **144**, 76–86 (2020).

40. Archibald, J. M. endosymbiosis and eukaryotic cell evolution. *Curr. Biol.* **25**, R911–R921 (2015).

41. Wang, X. et al. Mitochondrial flashes regulate ATP homeostasis in the heart. *Elife* **6**, e23908 (2017).

42. Fang, H. et al. Imaging superoxide flash and metabolism-coupled mitochondrial permeability transition in living animals. *Cell Res.* **21**, 1295–1304 (2011).

43. Fu, Z. X. et al. Dendritic mitoflash as a putative signal for stabilizing long-term synaptic plasticity. *Nat. Commun.* **8**, 31 (2017).

44. Ahmad, D. & Newman, E. B. A deficiency in cyclic AMP results in pH-sensitive growth of *Escherichia coli* K-12. *J. Bacteriol.* **170**, 3443–3447 (1988).

45. Grenier, F., Matteau, D., Baby, V. & Rodrigue, S. Complete genome sequence of *Escherichia coli* BW25113. *Genome Announc.* **2**, e01038–14 (2014).

46. Kulahoglu, C. & Brautigam, A. Quantitative transcriptome analysis using RNA-seq. *Methods Mol. Biol.* **1158**, 71–91 (2014).

47. Burton, N. A., Johnson, M. D., Antczak, P., Robinson, A. & Lund, P. A. Novel aspects of the acid response network of *E. coli* K-12 are revealed by a study of transcriptional dynamics. *J. Mol. Biol.* **401**, 726–742 (2010).

48. You, C. et al. Coordination of bacterial proteome with metabolism by cyclic AMP signalling. *Nature* **500**, 301–306 (2013).

49. Reddy, B. S. & Chatterji, B. N. An FFT-based technique for translation, rotation, and scale-invariant image registration. *IEEE Trans Image Process* **5**, 1266–1271 (1996).

50. Otsu, N. A Threshold Selection Method from Gray-Level Histograms. *IEEE Trans. Syst. Man Cybern.* **9**, 62–66 (1979).

51. Ahmad, M. B. & Tae-Sun, C. Local threshold and Boolean function based edge detection. *IEEE Trans. Consumer Electronics* **45**, 674–679 (1999).

52. Shafait, F., Keysers, D. & Breuel, T. M. In Electronic Imaging. 6 (SPIE) (2008).

53. Borgefors, G. Distance transformations in digital images. *Comput. Vis. Gr. Image Proc.* **34**, 344–371 (1986).

54. Vincent, L. & Soille, P. Watersheds in digital spaces: an efficient algorithm based on immersion simulations. *IEEE Trans. Pattern Anal. Mach. Intell.* **13**, 583–598 (1991).

55. Haris, K., Efstratiadis, S. N. & Maglaveras, N. In Proceedings 1998 International Conference on Image Processing. ICIP98 (Cat. No.98CB36269). 338–342 vol. 333.

56. Bleau, A. & Leon, L. J. Watershed-based segmentation and region merging. *Comput. Vis. Image Underst.* **77**, 317–370 (2000).